NEOPLASIA
www.neoplasia.com

Volume 18 Number 3 March 2016 pp. 142–151 142

Mesenchymal Stem Cells Promote Pancreatic Tumor Growth by Inducing Alternative Polarization of Macrophages[1,2]

Esha Mathew[*], Arthur L. Brannon[*,†], AnnaChiara Del Vecchio[‡], Paloma E. Garcia[§], Morgan K. Penny[¶], Kevin T. Kane[‡], Alekya Vinta[‡], Ronald J. Buckanovich[*,#] and Marina Pasca di Magliano[*,†,‡,]**

*Cellular and Molecular Biology Program, University of Michigan, Ann Arbor, MI, 48109; †Medical Scientist Training Program, University of Michigan, Ann Arbor, MI, 48109; ‡Department of Surgery, University of Michigan, Ann Arbor, MI, 48109; §Program in Pathology, University of Michigan, Ann Arbor, MI, 48109; ¶Program in Cancer Biology, University of Michigan, Ann Arbor, MI, 48109; #Department of Internal Medicine, University of Michigan, Ann Arbor, MI, 48109; **Department of Cell and Developmental Biology, University of Michigan, Ann Arbor, MI, 48109

Abstract

Pancreatic cancer is characterized by an extensive desmoplastic stroma, the functional relevance of which is poorly understood. Activated fibroblasts are a prevalent component of the stroma, and traditionally, these cells have been considered as a homogenous population derived from pancreatic stellate cells. In this study, we highlight a previously unappreciated heterogeneity of the fibroblast population within the stroma. In particular, a subset of stromal fibroblasts has characteristics of mesenchymal stem cells (MSCs). MSCs are present in the normal pancreas as well as in the carcinomatous pancreas (CA-MSCs). Here, we determine that CA-MSCs have increased tumor-promoting function compared with MSCs in normal pancreas. This ability to promote tumor growth is associated with CA-MSCs' unique ability to promote alternative macrophage polarization. Thus, our study identifies a previously uncharacterized cell population within the stroma and sheds light on tumor-promoting interactions between different components of the stroma.

Significance

Targeting the stroma is emerging as a new paradigm in pancreatic cancer; however, efforts to that effect are hampered by our limited understanding of the nature and function of stromal components. Here, we uncover previously unappreciated heterogeneity within the stroma and identify interactions among stromal components that promote tumor growth and could be targeted therapeutically.

Neoplasia (2016) 18, 142–151

Introduction

Pancreatic cancer is among the deadliest of human malignancies. A prominent feature of pancreatic cancer is an extensive reactive stroma, which can comprise up to 90% of the overall tumor volume, the highest fraction of all solid, epithelial tumors (for review, see [1]). The accumulation of a desmoplastic stroma occurs from the onset of pancreatic carcinogenesis and is evident in the precursor lesions of pancreatic cancer known as *pancreatic intraepithelial neoplasia* or *PanINs* [2]. The cellular components of the stroma include fibroblasts, myofibroblasts, endothelial cells, and infiltrating immune cells [3,4]. Fibroblasts are an abundant and poorly characterized component of the stroma, thought to derive from pancreatic stellate cells. Fibroblasts within the stroma have been thought of as protumor

Address all correspondence to: Marina Pasca di Magliano, PhD, Department of Surgery, University of Michigan, Ann Arbor, MI, 48109.
E-mail: marinapa@umich.edu

[1] This project was supported by the NCI-1R01CA151588-01and by an American Cancer Society Scholar grant to M. P. d. M. E. M. was supported by a University of Michigan Program in Cellular and Molecular Biology training grant (NIH T32 GM007315) and a University of Michigan Gastrointestinal Training grant (NIH T32 DK094775). A. L. B. was supported by a University of Michigan Warner-Lambert Rackham Fellowship.
Work in the Buckanovich laboratory was supported by NIH DP2004403 and 1-R01-CA163345-01.
[2] The authors declare they have no conflict of interest.
Received 15 January 2016; Accepted 25 January 2016

1476-5586
http://dx.doi.org/10.1016/j.neo.2016.01.005

agents [5], but recent studies have challenged this concept, indicating that stromal fibroblasts might act to restrain tumor growth [6,7]. This controversy might in part reflect our limited understanding of cellular components of the stroma and their individual contribution to tumorigenesis.

The healthy pancreas includes different fibroblast populations. A population of mesenchymal stem cells (P-MSCs) was identified in the normal human and mouse pancreas [8,9]; however, whether MSCs are present in pancreatic carcinoma and what their function might be during carcinogenesis remained unclear. MSCs were identified as a tumor-promoting stromal component in several epithelial cancers [10–12]. Interestingly, the manner in which MSCs promote tumorigenesis is distinct in each tumor context. In breast cancer, bone marrow–derived MSCs promote the metastasis of tumor cells through a CCL5-mediated effect [11]. In ovarian cancer, MSCs isolated from the tumor stroma secrete bone morphogenic proteins (BMPs) that increase the cancer stem cell population [12]. More recently, stroma-derived MSCs from lymphomas have been shown to secrete monocyte/macrophage chemoattractants, which in turn promote tumor growth [13].

The identification and characterization of MSCs in pancreatic tumor growth are the focus of the current study. We use a genetically engineered mouse model of pancreatic cancer, the KC mouse (Ptf1a-Cre;LSL-Kras^{G12D}) [14], that expresses an oncogenic form of Kras, thus recapitulating the most common genetic alteration in human PanINs and pancreatic cancer [15,16]. KC mice develop PanINs in a stepwise manner that recapitulates human carcinogenesis [14]. Our results show that MSC populations are present in both the normal murine pancreas (P-MSCs) and neoplastic mouse pancreas (carcinogenesis-associated MSCs, CA-MSCs). By performing functional comparisons of these two populations, we determined that CA-MSCs have an increased tumor-promoting potential, which is mediated, at least in part, by their unique ability to induce macrophage polarization to a protumor, alternatively activated status.

Results

MSCs in the Normal and in the Neoplastic Pancreas

MSCs are defined by their ability to differentiate into osteoblasts, chondrocytes, and adipocytes when exposed to appropriate differentiation media *in vitro*. To test whether we could identify an MSC population in the normal and neoplastic murine pancreas, we isolated pancreata from wild-type and littermate KC mice 3 weeks following caerulein-induced acute pancreatitis. Wild-type pancreata have completed the tissue repair process by this time, whereas in KC pancreata, extensive PanINs surrounded by desmoplastic stroma are evident (Figure 1*A*). Isolated bulk fibroblast populations from the pancreata were exposed to osteoblast, adipocyte, and chondrocyte differentiation media. Trilineage differentiation was observed both in the wild-type and in the KC-derived pancreata, indicating that an MSC population might exist in both settings (Figure 1*B*). Thus, our data confirmed the presence of an MSC population in the normal pancreas, as previously described [8,9,17], and identified a similar population in the neoplastic pancreas. MSCs have been isolated based on the expression of a panel of surface markers: CD45$^-$;CD44$^+$;-CD49a$^+$:CD73$^+$;CD90$^+$ [18]. To determine whether these markers were sufficient to isolate the MSC population in the pancreas, we isolated single-cell suspensions from wild-type and KC pancreata 3 weeks after the induction of pancreatitis (n = 3 mice/genotype) and used fluorescent-activated cell sorting to isolate and quantify cells expressing MSC markers. Although CD45$^-$;CD44$^+$;CD49a$^+$:CD73$^+$;CD90$^+$cells were present in both sample sets, their number was significantly higher in KC pancreata compared with the normal mouse pancreas (Figure 1*A*). To determine whether the surface markers did indeed identify the MSC population, we cultured CD44$^+$;CD49a$^+$:CD73$^+$;CD90$^+$ cells (putative MSCs, 4$^+$) as well as cells negative for all markers (4^{neg}) and performed *in vitro* differentiation assays with protocols promoting osteoblast and adipocyte lineages. In differentiation media, CD45$^-$;CD44$^+$;CD49a$^+$:CD73$^+$;CD90$^+$ cells from both the normal and neoplastic pancreas could differentiate into osteoblasts as determined by Alizarin Red staining of calcium deposits, and expression of the osteoblast marker alkaline phosphatase by quantitative reverse transcriptase polymerase chain reaction (qRT-PCR) analysis (Figure 1, *C* and *D*, *top row*). Likewise, CD45$^-$;CD44$^+$;CD49a$^+$:CD73$^+$;CD90$^+$ cells could differentiate into adipocytes as determined by Oil Red O staining of lipid droplets and expression of adipocyte marker fatty acid binding protein 4 (Fabp4) (Figure 1, *C* and *D, bottom row*). In contrast, 4^{neg} cells did not differentiate into any of the lineages (Figure 1, *C* and *D*), indicating that the combination of CD44$^+$, CD49a$^{+,}$ CD73$^+$ and CD90$^+$ surface markers identifies a subset of multipotent cells.

Distinct Cytokine Expression Profile in CA-MSCs

Because MSCs were present both in the normal and in the neoplastic pancreas, we set out to compare their functional characteristics. Hereby, normal pancreas–derived MSCs are referred to as *P-MSCs*, wherease MSCs derived from the neoplastic pancreas are referred to as *CA-MSCs* (carcinoma-associated MSCs). In ovarian cancer, CA-MSCs are distinct from bone marrow and adipose-derived MSCs by the expression of BMP2 and BMP4 [12], and those factors confer a higher tumor-promoting ability to CA-MSCs. Thus, we measured the relative expression of *BMP2* and *BMP4* by qRT-PCR in isolated P-MSCs and CA-MSCs. We detected no difference in *BMP2* expression, whereas *BMP4* expression was decreased in CA-MSCs compared with P-MSCs (Figure S1*A*).

We have previously shown that pancreatic fibroblasts secrete a number of cytokines that regulate the infiltration of immune cells during pancreatic damage and repair and during carcinogenesis [19]. Thus, we measured expression of those cytokines by qRT-PCR in freshly sorted P-MSCs and CA-MSCs. Interestingly, we observed a significant increase in several cytokines known to promote tumorigenesis, including *IL-6*, *IL-10*, and *TGFβ* [20–24] (Figure 1*E*), in CA-MSCs compared with P-MSCs. Then, we measured the expression of the same subset of cytokines in cultured CA-MSCs and P-MSCs, respectively, and found a similar profile, with significantly elevated cytokines in CA-MSCs (Figure S1*B*). Similarly *M-CSF* and *GM-CSF*, cytokines known to regulate immune cell recruitment and function, were significantly elevated in CA-MSCs compared with P-MSCs. Finally, we compared paired bone marrow and pancreatic MSCs extracted from a control mouse (P-BM MSCs and P-MSCs) or a PanIN-bearing KC mouse (CA-BM MSCs and CA-MSCs). P-MSCs expressed higher levels of *IL6, Cox-2,* and *IL10* than their bone marrow counterparts. CA-MSCs expressed higher levels of *IL6*, *Cox-2*, *TGFβ,* and *IL-10* than both P-MSCs and CA-BM MSCs (Figure S1**C**). These data indicate that MSCs extracted from the neoplastic pancreas have unique

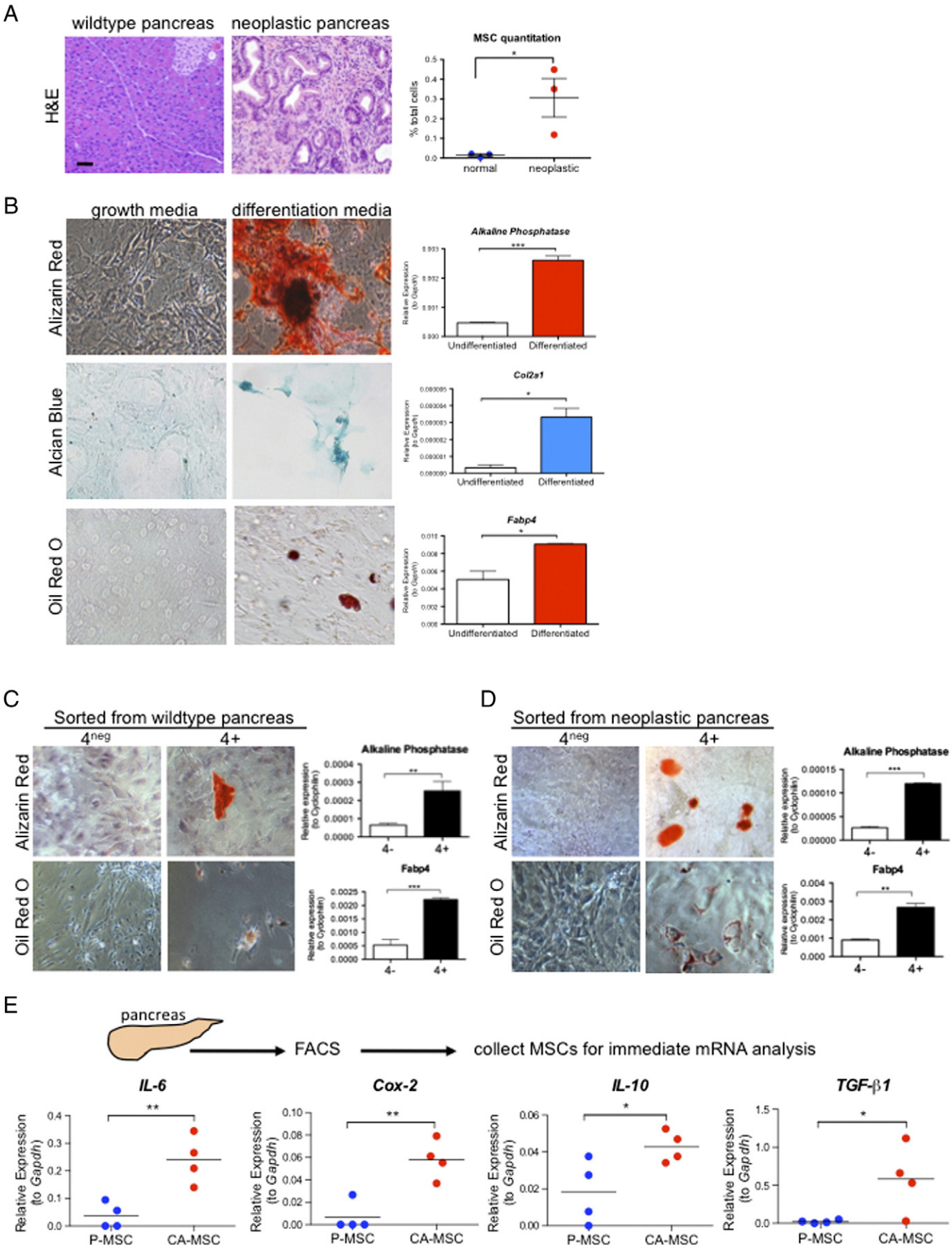

Figure 1. Multipotent stromal cells (MSCs) are present in the pancreas. (A) MSCs are increased in the neoplastic pancreas compared with the normal pancreas as quantified by flow cytometry. Scale bar for representative hematoxylin and eosin (H&E) images, 50 μm. (B) Stromal cells isolated from the neoplastic pancreas can differentiate into osteoblasts (top row), chondrocytes (middle row), and adipocytes (bottom row). (C) P-MSCs can differentiate into bone (top row) and fat (bottom row). (D) CA-MSCs can differentiate into bone (top row) and fat (bottom row). (E) qRT-PCR on MSCs freshly sorted from the pancreas.

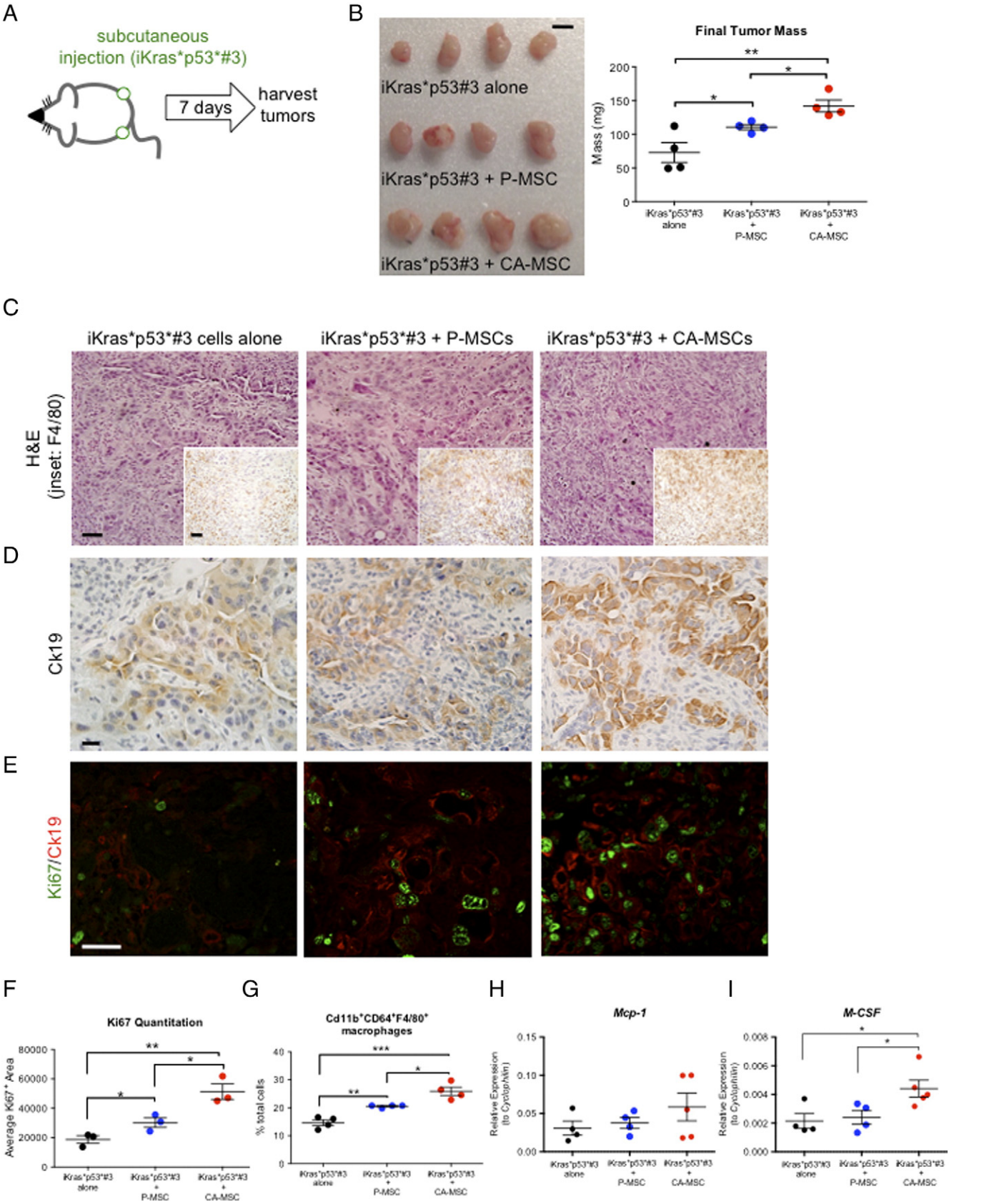

Figure 2. CA-MSCs promote tumor growth. (A) Experimental design. (B) Gross tumor morphology and final tumor weights. Scale bar represents 0.5 cm. (C) Histopathological analysis of tumors following coinjection. H&E staining; scale bar represents 50 μm. (Inset) F4/80 staining; scale bar represents 50 μm. (D) Immunohistochemistry for Ck19; scale bar represents 20 μm. (E) Immunohistochemistry for Ki67 (green) and Ck19 (red); scale bar represents 20 μm. (F) Quantitation of Ki67 staining. (G) Flow cytometry analysis of macrophages. (H) qRT-PCR analysis for *Mcp-1* and (I) *M-csf*.

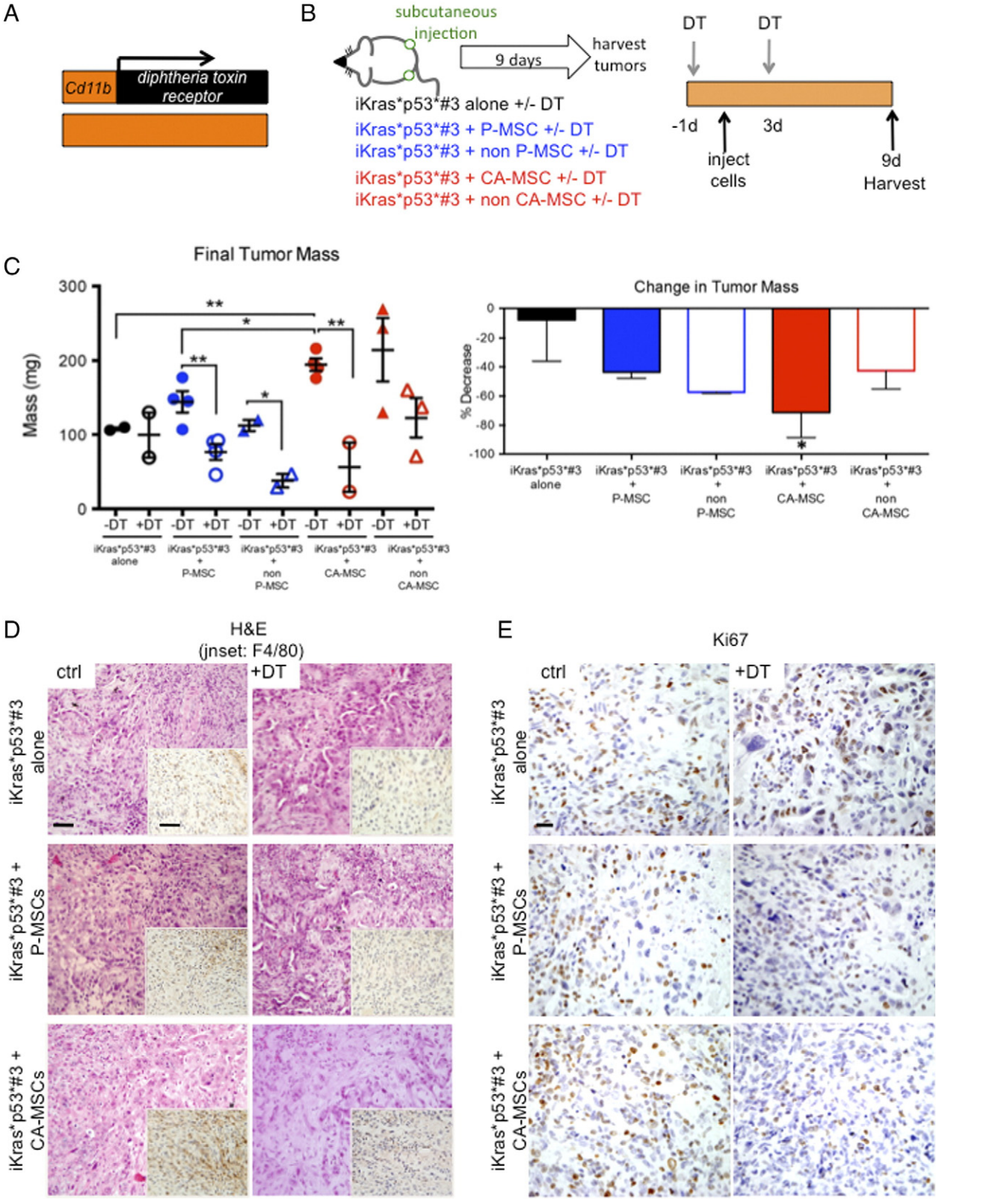

Figure 3. Myeloid cells are vital for CA-MSC–mediated tumor growth. (A) Schematic for Cd11b-DTR mouse. (B) Experimental design. (C, Left) Final tumor weights. Data are presented as mean ± SEM. (Right) Percentage decrease in tumor weights. (D) Histopathological analysis of tumors following coinjection. H&E staining; scale bar represents 50 μm. (Inset) F4/80 staining; scale bar represents 50 μm. (E) Immunohistochemistry for Ki67; scale bar represents 20 μm.

characteristics that are not shared by their counterpart extracted from the normal organ nor by MSCs extracted by different organs (in this case, the bone marrow) of a mouse bearing neoplastic changes in the pancreas.

MSCs Pancreatic Tumor Growth

To determine the functional effect of MSCs on tumor growth, we performed subcutaneous coinjections of tumor cells and MSCs into immunocompetent mice using a littermate syngeneic approach. We used tumor cells isolated from the iKras*p53* model [25] of pancreatic cancer (iKras*p53*#3 cells [26]) or tumor cells derived from the KPC mouse model [27] of pancreatic cancer (13442 cells). Tumor cells were injected at a 1:1 ratio with either P-MSCs or CA-MSCs (see schematic in Figures 2*A* and S2*A*). Coinjection of P-MSCs with iKras*p53*#3 or 13442 tumor cells promoted tumor growth, but coinjection of CA-MSCs promoted even larger tumor growth (Figures 2*B* and S2*B*). The histology of all three cohorts was similar, with epithelial structures surrounded by abundant stroma (Figures 2*C* and S2*C*). Staining for Ck19 to mark tumor cells revealed increased number of tumor cells in coinjections with CA-MSCs (Figures 2*D* and S2*D*). Consistently, we detected increased intratumor proliferation—as indicated by Ki67 staining—in coinjections with CA-MSCs. Immunofluorescence analysis revealed a notable increase in proliferating tumor Ck19+ cells, indicating an increase in proliferating tumor cells (Figures 2, *E* and *F,* and S2, *D* and **E**). To determine whether MSCs were still able to promote tumor growth when injected at a lower ratio, we performed a parallel set of experiments by injecting tumor cells (13442) and MSCs at a 2:1 ratio. We found that, at this lower ratio, P-MSCs were unable to promote tumor growth, whereas in contrast, CA-MSCs still promoted tumor growth, further validating the concept that CA-MSCs have increased tumor-promoting ability (Figure S2*K*).

Because our data indicated that CA-MSCs have different functional characteristics than P-MSC, we expanded our characterization to include bone marrow–derived MSCs (BM-MSCs). In the absence of rigorous lineage tracing studies, it is not known whether CA-MSCs derived from P-MSCs or, at least in part, from infiltrating BM-MSCs, as observed in other disease contexts [28,29]. This is a question that warrants further studies that are beyond the scope of the current manuscript. BM-MSCs from a control mouse promoted tumor growth similarly to P-MSCs. However, CA-MSCs were able to promote significantly more tumor growth than their bone marrow–derived counterparts (Figure S2, *I* and *J*). Thus, CA-MSCs have a unique tumor promoting ability; we then set out to understand the mechanistic basis for this finding.

Given our previous observation that CA-MSCs secreted a number of cytokines that are known to regulate macrophages, we sought to determine the effect of MSC coinjection on macrophage infiltration within the tumor. Thus, we stained tissues for F4/80, a mature macrophage marker. We detected a significant increase in macrophages in the tumors derived from coinjection of tumor cells and CA-MSCs (Figures 2*C* and S2*C*, *insets*) compared with tumor cells alone or coinjected with P-MSCs. To quantify macrophage numbers in the subcutaneous tumors, we performed flow cytometry for macrophages defined as $CD11b^+$;$CD64^+$;$F4/80^+$ cells. We found that tumors derived from the CA-MSC coinjection consistently had the highest population of macrophages compared with the other experimental cohorts, thus corroborating the histology (Figures 2*G* and S2*F*).

Monocyte migration to the tumor stroma and subsequent differentiation into macrophages are processes orchestrated by an array of signaling molecules. To assess potential differences in these cytokine levels between tumor cohorts, we collected RNA from subcutaneous tumor tissue for qRT-PCR analysis. We found that expression of *Mcp-1*, a potent monocyte chemoattractant, did not differ between tumors coinjected with P-MSCs or with CA-MSCs but, at least for tumors derived from the 13442 line, was higher in the MSC-coinjected tumors than in the control group (Figures 2*H* and S2*G*). Interestingly, we detected an increase in M-CSF in coinjections with CA-MSCs (Figures 2*I* and S2*H*), a cytokine that supports the differentiation of monocytes into macrophages.

Requirement for Monocytes/Macrophages in MSC-driven tumor growth

Macrophages have been shown to promote pancreatic growth [30]. Thus, based on the observation that CA-MSCs promoted the highest infiltration of macrophages, we next tested whether this population's elevated tumor-promoting potential *required* macrophages. To achieve this, we coinjected tumor cells and MSCs into immunocompetent mice with concomitant depletion of monocytes and macrophages. Cd11b-DTR mice express the human diphtheria toxin receptor under the Cd11b promoter (Figure 3*A*). Administration of diphtheria toxin (DT) to Cd11b-DTR mice depletes all CD11b+ cells, including monocytes and macrophages [31]. We performed a series of coinjection experiments with iKras*p53*#3 cells alone or in combination with P-MSCs or CA-MSCs. In a subset of each cohort, mice were injected with DT (Figure 3*B*). We confirmed DT-mediated depletion by staining tumor tissues for F4/80; in all cohorts, DT administration significantly attenuated macrophage infiltration (Figure 3*D*, *inset*). We found that tumor size was reduced by depleting CD11b+ cells in all experimental cohorts, underscoring the importance of myeloid cells in tumor growth. However, coinjections of iKras*p53*#3 cells with CA-MSCs were significantly more susceptible to myeloid cell ablation than any other experimental cohort, both in terms of tumor mass changes (Figure 3*C*) and when considering the ratio of epithelial cells within the tumor (Figure 3*D*). The susceptibility of CA-MSCs to myeloid cell depletion was consistently observed using distinct MSC lines (Figure S3*D*). Whereas the tumor histology remained similar (Figure 3*D*), immunostaining for Ck19 revealed a reduction in the ratio of epithelial cells within the tumors (Figure S3*A*). Moreover, although tumors derived from coinjections with CA-MSCs are more proliferative than the other cohorts, this increase in proliferation was abrogated upon myeloid cell depletion (Figure 3*E*).

To determine whether the dependence on myeloid cells for tumor promotion was a unique property of CA-MSCs or rather a common feature of fibroblasts derived from the neoplastic pancreas, we performed parallel coinjection experiments with non-MSCs ($CD45^-$;$CD44^-$;$CD49a^-$:$CD73^-$;$CD90^-$) sorted from the neoplastic stroma (CA-non-MSCs) (Figure S3*B*). Although these cells also promoted tumor growth, the extent of tumor mass reduction upon CD11b+ cell depletion was less than in coinjections with MSCs (Figure S3*C*). Thus, CA-MSCs have a unique dependence on myeloid cells, which led us to investigate the interaction between these cell types.

MSCs Promote Macrophage Differentiation and Polarization to an Alternatively Activated Subtype

Pancreatic cancer fibroblasts, including the FAP+ subset, are known to modulate the immune response, thus affecting tumor growth [32,33]. To directly interrogate whether MSCs directly regulate macrophage polarization, we investigated their interactions

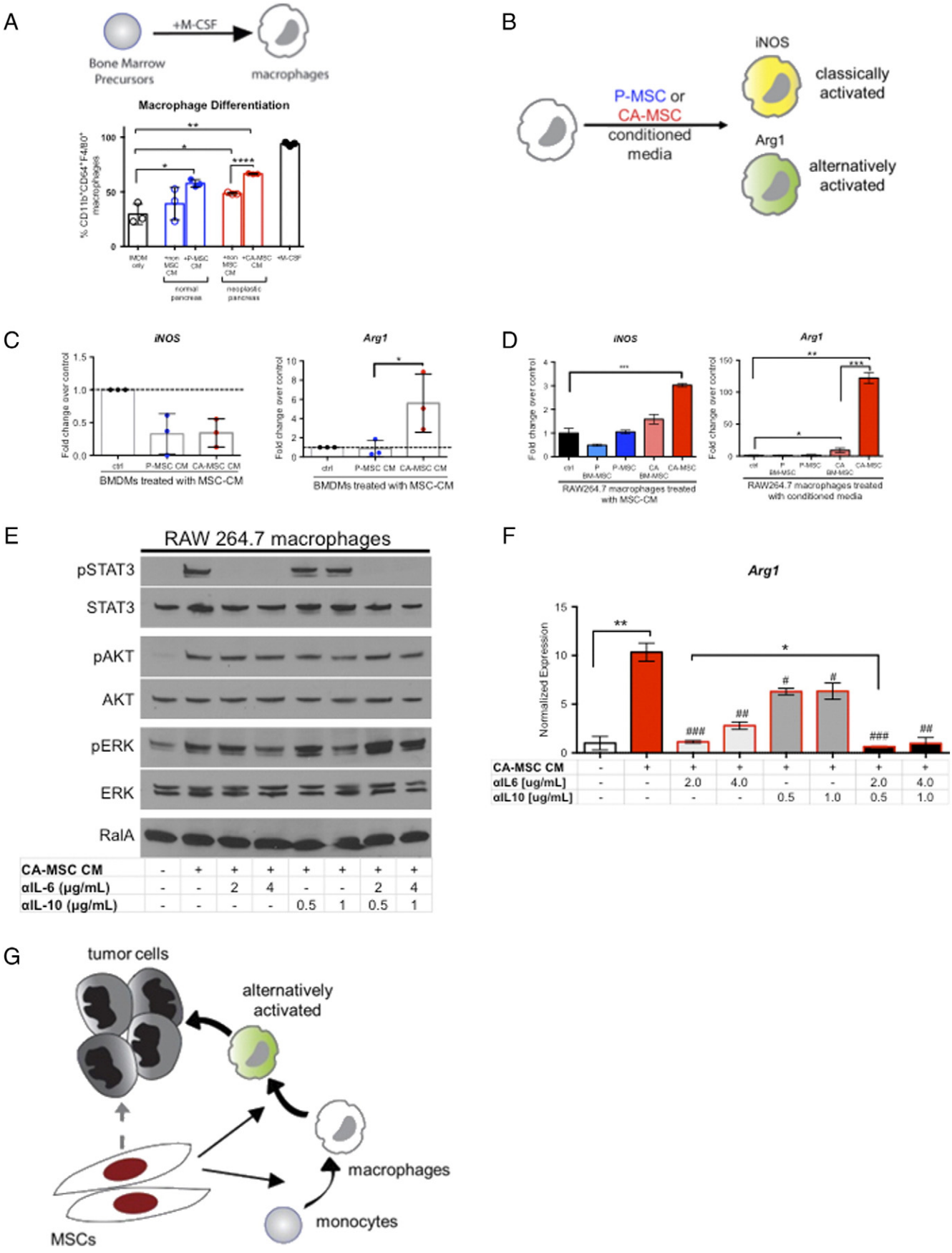
A
+M-CSF
Bone Marrow Precursors
macrophages
Macrophage Differentiation
% CD11b+CD64+F4/80+ macrophages
BMDM only
+non MSC CM
+P-MSC CM
+CA-MSC CM
+M-CSF
normal pancreas
neoplastic pancreas
B
P-MSC or CA-MSC conditioned media
iNOS
classically activated
Arg1
alternatively activated
C
iNOS
Arg1
Fold change over control
ctrl
P-MSC CM
CA-MSC CM
BMDMs treated with MSC-CM
D
iNOS
Arg1
Fold change over control
ctrl
P BM-MSC
P-MSC
CA BM-MSC
CA-MSC
RAW264.7 macrophages treated with MSC-CM
RAW264.7 macrophages treated with conditioned media
E
RAW 264.7 macrophages
pSTAT3
STAT3
pAKT
AKT
pERK
ERK
RalA
CA-MSC CM - + + + + + + +
αIL-6 (μg/mL) - - 2 4 - - 2 4
αIL-10 (μg/mL) - - - - 0.5 1 0.5 1
F
Arg1
Normalized Expression
CA-MSC CM - + + + + + + +
αIL6 [ug/mL] - - 2.0 4.0 - - 2.0 4.0
αIL10 [ug/mL] - - - - 0.5 1.0 0.5 1.0
G
tumor cells
alternatively activated
macrophages
monocytes
MSCs

in vitro. First, we sought to determine whether CA-MSCs promote the differentiation of monocytes into macrophages. For this purpose, we isolated and cultured mouse bone marrow precursors. After 1 week of culture in regular medium, about 25% of the cell population differentiates to macrophages, defined as $CD11b^+;CD64^+;F4/80^+$ cells by flow cytometry. As expected based on previous studies [34], exposure to M-CSF–supplemented media led to differentiation of a uniform population of $CD11b^+;CD64^+;F4/80^+$ macrophages (Figure 4*A*). We tested the effect of supplementing the culture medium with conditioned media from either P-MSCs or CA-MSCs, as well as P-non-MSCs and CA-non-MSCs (pancreatic fibroblasts or neoplastic fibroblasts). Both P-MSCs and CA-MSCs promoted macrophage differentiation in more than 50% of the bone marrow precursors, with no significant difference between the two populations. In contrast, only non-MSC fibroblasts from the neoplastic pancreas could also promote macrophage differentiation, although to a lesser extent than their MSC counterparts (Figure 4*A*).

We next assessed whether P-MSCs or CA-MSCs regulated macrophage polarization. First, we performed qRT-PCR to evaluate gene expression indicating either classically or alternatively activated macrophage polarization RNA collected from our subcutaneous coinjection experiments (Figure S4, *A* and *B*). We found that tumors derived from coinjection with both P-MSCs and CA-MSCs had decreased expression of *iNos*, a classically activated marker, compared with tumor cells injected alone. However, only coinjections with CA-MSCs tumor cells showed increased expression of *Arg1* and *CD206*, both markers of alternatively activated macrophages. Likewise, the expression of IL10, a cytokine known to induce alternative macrophage differentiation, was significantly increased in coinjections with CA-MSCs (Figure S4, *A* and *B*). Importantly, these changes were observed with both iKras*p53* and KPC tumor cells.

To test whether MSCs directly regulated macrophage polarization to an alternatively activated phenotype, we treated three independently derived cultures of bone marrow–derived macrophages (BMDMs) with conditioned media from either P-MSCs or CA-MSCs for 12 hours (Figure 4*B*). We found that both P-MSC– and CA-MSC–conditioned media decreased *iNOS* expression in BMDMs compared with control medium, indicating suppression of the classically activated subtype. However, only CA-MSC–conditioned medium promoted alternatively activated macrophage polarization, as determined by *Arg1* expression (Figure 4*C*). We then repeated this set of experiments using the mouse macrophage cell line RAW264.7 that can be polarized in culture. Conditioned medium from P-MSCs had no effect on the expression of *iNos* or *Arg1* in macrophages. In contrast, whereas conditioned medium from CA-MSCs stimulated a four-fold increase in *iNos* expression, *Arg1* expression was increased more than one-hundred–fold. We also tested the effect of conditioned media from bone marrow MSCs, which have been reported to induce *Arg1* expression in macrophages, leading to an alternatively activated phenotype [35,36]. We found that whereas CA BM-MSCs could promote *Arg1* expression, this effect was significantly less than CA-MSCs (Figure 4*D*). Likewise, CA-MSCs could stimulate significantly greater *Arg1* expression than CAFs (non–CA-MSCs) (Figure S4*C*). Taken together, our data indicate that the ability to promote alternatively activated macrophage polarization is restricted to CA-MSCs.

As CA-MSCs expressed significantly higher *IL-6* and *IL-10* compared with P-MSCs and these cytokines are known to regulate macrophage polarization, we tested whether production of these cytokines explained the unique ability of CA-MSCs to promote macrophage alternative activation. Thus, we treated RAW264.7 macrophages with CA-MSC conditioned media with and without an IL-6–neutralizing antibody or an IL-10–neutralizing antibody and assessed *Arg1* expression. Consistent with IL-6 stimulation, CA-MSC conditioned medium increased pSTAT3(Y705) levels in RAW264.7 macrophages compared with control medium, and this increase was abrogated by the anti-IL6 antibody but not by the anti-IL10 antibody (Figure 4*E*). Treatment with CA-MSC conditioned medium induced *Arg1* expression in RAW264.7 macrophages; this induction was partially abrogated by anti-IL6 and, to a lesser extent, by anti-IL10 treatment (Figure 4*F*). Concomitant treatment with anti-IL6 and anti-IL10 antibodies completely blocked the induction of *Arg1* expression, indicating that these two cytokines might act along parallel, nonoverlapping paths. We then investigated the effect of CA-MSC conditioned medium on the expression of classically activated differentiation markers. We observed no change in *iNOS* expression but a reduction of *IL12p35* upon treatment with conditioned medium (Figure S4, *D* and *E*). This decrease was reversed with higher concentrations of either IL6 or IL10 inhibition. Taken together, our results show that both P-MSCs and CA-MSCs can induce macrophage differentiation for a precursor population, but only CA-MSCs specifically direct polarization to a tumor-promoting, alternatively activated subtype.

Discussion

Fibroblasts exist in every tissue and organ in the body and are a prevalent population within the pancreatic cancer stroma. Our understanding of their functional specificity, however, remains limited. Here, we have identified a subpopulation of fibroblasts present both within the normal pancreas and in the neoplastic pancreas, with MSC characteristics, namely, the ability to differentiate into chondrocytes, adipocytes, and osteoblasts. We determined that MSCs from the neoplastic pancreas (CA-MSCs) have a unique ability to promote tumor growth that depends on their ability to promote infiltration of monocytes/macrophages and their differentiation to an alternatively activated, tumor-promoting, phenotype (Figure 4*G*). Our study highlights the functional heterogeneity of stromal fibroblast populations and the different functional properties of fibroblasts derived from the normal or neoplastic organ. Furthermore, our study identifies novel interactions between the fibroblast population and the immune component of pancreatic cancer.

Figure 4. CA-MSC–derived IL6 and IL10 promote alternatively activated macrophage polarization. (A) Flow cytometry analysis of *in vitro* differentiated macrophages. Each data point represents bone marrow precursors from one mouse. (B) Experimental design. (C) qRT-PCR on BMDMs for *iNOS* (left) and *Arg1* (right). Each data point represents BMDMs from one mouse. (D) qRT-PCR on Raw264.7 macrophages for *iNOS* (left) and *Arg1* (right). (E) Western blot analysis of RAW264.7 macrophages treated with conditioned media and inhibitors. (F) qRT-PCR on RAW264.7 macrophages treated with conditioned media and inhibitors for *Arg1*. # indicates significant differences from CA-MSC–stimulated cells. (G) Working model of CA-MSC–mediated promotion of tumor growth.

Experimental Procedures

Detailed reagent information and experimental procedures are provided in Supplemental Experimental Procedures.

Statistical Analysis

Student's *t* tests were used to compare experimental cohorts, and significance was established for *P* values < .05. Significance values indicated by asterisks or pound signs are as follows: $^{*}P < .05$, $^{**}P < .01$, $^{***}P < .0005$, and $^{****}P < .0001$.

Author Contributions

E. M. and M. P. d. M. conceived and designed the experiments. E. M. executed the experiments and collected the data. A. L. B., A. d. V., M. K. P., K. T. K., P. E. G., and A. d. V. assisted with data collection and analysis. R. J. B. provided expertise on the identification and characterization of MSC in the cancer stroma and shared protocols and reagents developed in his laboratory. E. M., A. L. B., P. E. G., and M. P. d. M. wrote and edited the manuscript.

Supplementary data to this article can be found online at http://dx.doi.org/10.1016/j.neo.2016.01.005.

Acknowledgements

This project was supported by the NCI-1R01CA151588-01 to M. P. d. M. E. M. was supported by a University of Michigan Program in Cellular and Molecular Biology training grant (NIH T32 GM007315) and a University of Michigan Gastrointestinal Training grant (NIH T32 DK094775). A. L. B. was supported by a University of Michigan Warner-Lambert Rackham Fellowship. The authors declare they have no conflict of interest. We would like to thank G. Martinez-Santibañez and C. Lumeng for protocols and reagents for macrophage experiments. We also thank L. Cabrera for technical advice and reagents for MSC differentiation experiments.

References

[1] Neesse A, Michl P, Frese KK, Feig C, Cook N, Jacobetz MA, Lolkema MP, Buchholz M, Olive KP, and Gress TM, et al (2011). Stromal biology and therapy in pancreatic cancer. *Gut* **60**, 861–868.

[2] Hruban RH, Maitra A, and Goggins M (2008). Update on pancreatic intraepithelial neoplasia. *Int J Clin Exp Pathol* **1**, 306–316.

[3] Clark CE, Hingorani SR, Mick R, Combs C, Tuveson DA, and Vonderheide RH (2007). Dynamics of the immune reaction to pancreatic cancer from inception to invasion. *Cancer Res* **67**, 9518–9527.

[4] Apte MV, Park S, Phillips PA, Santucci N, Goldstein D, Kumar RK, Ramm GA, Buchler M, Friess H, and McCarroll JA, et al (2004). Desmoplastic reaction in pancreatic cancer: role of pancreatic stellate cells. *Pancreas* **29**, 179–187.

[5] Hwang RF, Moore T, Arumugam T, Ramachandran V, Amos KD, Rivera A, Ji B, Evans DB, and Logsdon CD (2008). Cancer-associated stromal fibroblasts promote pancreatic tumor progression. *Cancer Res* **68**, 918–926.

[6] Ozdemir BC, Pentcheva-Hoang T, Carstens JL, Zheng X, Wu CC, Simpson TR, Laklai H, Sugimoto H, Kahlert C, and Novitskiy SV, et al (2014). Depletion of carcinoma-associated fibroblasts and fibrosis induces immunosuppression and accelerates pancreas cancer with reduced survival. *Cancer Cell* **25**, 719–734.

[7] Rhim AD, Oberstein PE, Thomas DH, Mirek ET, Palermo CF, Sastra SA, Dekleva EN, Saunders T, Becerra CP, and Tattersall IW, et al (2014). Stromal elements act to restrain, rather than support, pancreatic ductal adenocarcinoma. *Cancer Cell* **25**, 735–747.

[8] Baertschiger RM, Bosco D, Morel P, Serre-Beinier V, Berney T, Buhler LH, and Gonelle-Gispert C (2008). Mesenchymal stem cells derived from human exocrine pancreas express transcription factors implicated in beta-cell development. *Pancreas* **37**, 75–84.

[9] Crisan M, Yap S, Casteilla L, Chen CW, Corselli M, Park TS, Andriolo G, Sun B, Zheng B, and Zhang L, et al (2008). A perivascular origin for mesenchymal stem cells in multiple human organs. *Cell Stem Cell* **3**, 301–313.

[10] Joyce JA and Pollard JW (2009). Microenvironmental regulation of metastasis. *Nat Rev Cancer* **9**, 239–252.

[11] Karnoub AE, Dash AB, Vo AP, Sullivan A, Brooks MW, Bell GW, Richardson AL, Polyak K, Tubo R, and Weinberg RA (2007). Mesenchymal stem cells within tumour stroma promote breast cancer metastasis. *Nature* **449**, 557–563.

[12] McLean K, Gong Y, Choi Y, Deng N, Yang K, Bai S, Cabrera L, Keller E, McCauley L, and Cho KR, et al (2011). Human ovarian carcinoma-associated mesenchymal stem cells regulate cancer stem cells and tumorigenesis via altered BMP production. *J Clin Invest* **121**, 3206–3219.

[13] Ren G, Zhao X, Wang Y, Zhang X, Chen X, Xu C, Yuan ZR, Roberts AI, Zhang L, and Zheng B, et al (2012). CCR2-dependent recruitment of macrophages by tumor-educated mesenchymal stromal cells promotes tumor development and is mimicked by TNFalpha. *Cell Stem Cell* **11**, 812–824.

[14] Hingorani SR, Petricoin EF, Maitra A, Rajapakse V, King C, Jacobetz MA, Ross S, Conrads TP, Veenstra TD, and Hitt BA, et al (2003). Preinvasive and invasive ductal pancreatic cancer and its early detection in the mouse. *Cancer Cell* **4**, 437–450.

[15] Biankin AV, Waddell N, Kassahn KS, Gingras MC, Muthuswamy LB, Johns AL, Miller DK, Wilson PJ, Patch AM, and Wu J, et al (2012). Pancreatic cancer genomes reveal aberrations in axon guidance pathway genes. *Nature* **491**, 399–405.

[16] Jones S, Zhang X, Parsons DW, Lin JC, Leary RJ, Angenendt P, Mankoo P, Carter H, Kamiyama H, and Jimeno A, et al (2008). Core signaling pathways in human pancreatic cancers revealed by global genomic analyses. *Science* **321**, 1801–1806.

[17] Gopurappilly R, Bhat V, and Bhonde R (2013). Pancreatic tissue resident mesenchymal stromal cell (MSC)–like cells as a source of in vitro islet neogenesis. *J Cell Biochem* **114**, 2240–2247.

[18] Dominici M, Le Blanc K, Mueller I, Slaper-Cortenbach I, Marini F, Krause D, Deans R, Keating A, Prockop D, and Horwitz E (2006). Minimal criteria for defining multipotent mesenchymal stromal cells. The International Society for Cellular Therapy position statement. *Cytotherapy* **8**, 315–317.

[19] Mathew E, Collins MA, Fernandez-Barrena MG, Holtz AM, Yan W, Hogan JO, Tata Z, Allen BL, Fernandez-Zapico ME, and di Magliano MP (2014). The transcription factor GLI1 modulates the inflammatory response during pancreatic tissue remodeling. *J Biol Chem* **289**, 27727–27743.

[20] Lesina M, Kurkowski MU, Ludes K, Rose-John S, Treiber M, Kloppel G, Yoshimura A, Reindl W, Sipos B, and Akira S, et al (2011). Stat3/Socs3 activation by IL-6 transsignaling promotes progression of pancreatic intraepithelial neoplasia and development of pancreatic cancer. *Cancer Cell* **19**, 456–469.

[21] Zhang Y, Yan W, Collins MA, Bednar F, Rakshit S, Zetter BR, Stanger BZ, Chung I, Rhim AD, and di Magliano MP (2013). Interleukin-6 is required for pancreatic cancer progression by promoting MAPK signaling activation and oxidative stress resistance. *Cancer Res* **73**, 6359–6374.

[22] Sharma S, Stolina M, Lin Y, Gardner B, Miller PW, Kronenberg M, and Dubinett SM (1999). T cell-derived IL-10 promotes lung cancer growth by suppressing both T cell and APC function. *J Immunol* **163**, 5020–5028.

[23] Amatangelo MD, Goodyear S, Varma D, and Stearns ME (2012). c-Myc expression and MEK1-induced Erk2 nuclear localization are required for TGF-beta induced epithelial-mesenchymal transition and invasion in prostate cancer. *Carcinogenesis* **33**, 1965–1975.

[24] Yeh TS, Wu CW, Hsu KW, Liao WJ, Yang MC, Li AF, Wang AM, Kuo ML, and Chi CW (2009). The activated Notch1 signal pathway is associated with gastric cancer progression through cyclooxygenase-2. *Cancer Res* **69**, 5039–5048.

[25] Collins MA, Brisset JC, Zhang Y, Bednar F, Pierre J, Heist KA, Galban CJ, Galban S, and di Magliano MP (2012). Metastatic pancreatic cancer is dependent on oncogenic Kras in mice. *PLoS One* **7**, e49707.

[26] Jiang W, Zhang Y, Kane KT, Collins MA, Simeone DM, di Magliano MP, and Nguyen KT (2015). CD44 regulates pancreatic cancer invasion through MT1-MMP. *Mol Cancer Res* **13**, 9–15.

[27] Hingorani SR, Wang L, Multani AS, Combs C, Deramaudt TB, Hruban RH, Rustgi AK, Chang S, and Tuveson DA (2005). Trp53R172H and KrasG12D cooperate to promote chromosomal instability and widely metastatic pancreatic ductal adenocarcinoma in mice. *Cancer Cell* **7**, 469–483.

[28] Quante M, Tu SP, Tomita H, Gonda T, Wang SS, Takashi S, Baik GH, Shibata W, Diprete B, and Betz KS, et al (2011). Bone marrow–derived myofibroblasts contribute to the mesenchymal stem cell niche and promote tumor growth. *Cancer Cell* **19**, 257–272.

[29] Kramann R, Schneider RK, DiRocco DP, Machado F, Fleig S, Bondzie PA, Henderson JM, Ebert BL, and Humphreys BD (2015). Perivascular Gli1+ progenitors are key contributors to injury-induced organ fibrosis. *Cell Stem Cell* **16**, 51–66.

[30] Zhu Y, Knolhoff BL, Meyer MA, Nywening TM, West BL, Luo J, Wang-Gillam A, Goedegebuure SP, Linehan DC, and DeNardo DG (2014). CSF1/CSF1R blockade reprograms tumor-infiltrating macrophages and improves response to T-cell checkpoint immunotherapy in pancreatic cancer models. *Cancer Res* **74**, 5057–5069.

[31] Duffield JS, Forbes SJ, Constandinou CM, Clay S, Partolina M, Vuthoori S, Wu S, Lang R, and Iredale JP (2005). Selective depletion of macrophages reveals distinct, opposing roles during liver injury and repair. *J Clin Invest* **115**, 56–65.

[32] Feig C, Jones JO, Kraman M, Wells RJ, Deonarine A, Chan DS, Connell CM, Roberts EW, Zhao Q, and Caballero OL, et al (2013). Targeting CXCL12 from FAP-expressing carcinoma-associated fibroblasts synergizes with anti-PD-L1 immunotherapy in pancreatic cancer. *Proc Natl Acad Sci U S A* **110**, 20212–20217.

[33] Erez N, Truitt M, Olson P, Arron ST, and Hanahan D (2010). Cancer-associated fibroblasts are activated in incipient neoplasia to orchestrate tumor-promoting inflammation in an NF-kappaB–dependent manner. *Cancer Cell* **17**, 135–147.

[34] Weischenfeldt J and Porse B (2008). Bone marrow–derived macrophages (BMM): isolation and applications. CSH Protoc 2008, pdb prot5080; 2008 .

[35] Cho DI, Kim MR, Jeong HY, Jeong HC, Jeong MH, Yoon SH, Kim YS, and Ahn Y (2014). Mesenchymal stem cells reciprocally regulate the M1/M2 balance in mouse bone marrow–derived macrophages. *Exp Mol Med* **46**, e70.

[36] Zhang QZ, Su WR, Shi SH, Wilder-Smith P, Xiang AP, Wong A, Nguyen AL, Kwon CW, and Le AD (2010). Human gingiva-derived mesenchymal stem cells elicit polarization of m2 macrophages and enhance cutaneous wound healing. *Stem Cells* **28**, 1856–1868.